JMEPEG (2015) 24:3400–3406
DOI: 10.1007/s11665-015-1624-9

1059-9495/$19.00

Quantitative Image Analysis of Ni-P Coatings Deposited on Carbon Fibers

R. Kozera, J.J. Bucki, A. Sałacińska, J. Bieliński, and A. Boczkowska

(Submitted December 31, 2014; in revised form May 16, 2015; published online July 22, 2015)

In this work, polyacrylonitrile (PAN)-based carbon fibers coated with different thicknesses of Ni-P coatings were studied. The coatings were deposited by electroless metallization lasting from 3 to 22 min and consisted of approximately 3 wt.% phosphorous. Computer quantitative image analysis was used to characterize the surface features and thickness of the coatings as a function of the time of metallization. The results showed that quantitative image analysis is a useful technique for the measurement of the coating thickness and can be used as a tool for obtaining an innovative description of the Ni-P coating morphology. The morphology of the coatings and their thicknesses were investigated by scanning electron microscopy. The image analyses were performed using the proprietary software Micrometer, developed at the Faculty of Materials Science and Engineering, Warsaw University of Technology. The observations revealed that a specific feature of the coating topography is the hemispherical bulge of a diameter ranging from 0.1 to 10 μm. The thickness of the coatings increases linearly with the metallization time. The obtained results indicated that the methodology proposed in the present work can be successfully applied and possesses several advantages over the traditionally used weight measurements technique.

Keywords carbon fibers, electroless process, image analysis, Ni-P coatings

1. Introduction

Nickel-phosphorus coatings are widely used due to their unique chemical and mechanical properties. Among the advantages, the most important are good corrosion and wear resistance and high hardness. For these reasons, Ni-P layers are used in micro-galvanic and optical applications and in the automotive industry as protective layers (Ref 1-3). The most popular techniques for obtaining these types of coatings are: electro- and electroless plating. Despite a few drawbacks (high amount of waste and the complex composition of the solution), the electroless technique exhibits several advantages. In particular, it allows uniform coating on non-conductive surfaces with complicated geometry (Ref 3, 4), especially on bundles of carbon fibers, which when coated with Ni-P layers are used in polymer matrix composites for electromagnetic shielding (Ref 5-9). Moreover, Ni-P layers on carbon fiber scan be used to fabricate reinforced metal matrix composites (Ref 10-12) because they increase the wettability between the fiber and the metal (Ref 13-16). The properties of Ni-P coatings on carbon fibers were described in previous research (Ref 17-19). However, their morphology and thickness were not addressed in a comprehensive way. In particular, the thickness of the coatings was estimated globally by measuring the weight of deposited Ni. The results of the morphology investigation presented in the presented paper can be correlated with the wettability tests of the coatings using liquid alloy droplets, where the coating morphology and roughness play crucial roles. This gives support to the efforts aimed at the quantitative characterization of the coating based on their images, the results of which are reported in this paper. A literature survey indicated that there has been no attempt to parameterize these features quantitatively or to demonstrate the dependence of the time of the metallization process on the function of the thickness of Ni-P coatings and the diameter of their hemispheres. The authors of this paper attempted to perform this task by computer quantitative image analysis.

R. Kozera, J.J. Bucki, A. Sałacińska, and **A. Boczkowska**, Faculty of Materials Science and Engineering, Warsaw University of Technology, Woloska Str 141, 02-507 Warsaw, Poland; and **J. Bieliński**, Faculty of Chemistry, Warsaw University of Technology, Noakowskiego Str 3, 00-664 Warsaw, Poland. Contact e-mail: rafal.kozera@inmat.pw.edu.pl.

2. Experimental

The polyacrylonitrile (PAN)-based carbon fibers used in this work were Tenax HTA40, in bundles containing 3 K fibers with a diameter of 7 μm. The continuous fibers were cut into 11 cm pieces. The protective epoxy layer (sizing) deposited on the fibers by the manufacturer was removed by annealing in an oven for 1 h at 450 °C in an air atmosphere. The fiber surface preparation process for further metallization consisted of three stages: (1) sensitization, (2) activation, and (3) pre-reduction. The fibers were sensitized for 15 min in a solution consisting of $SnCl_2$ and HCl. Afterwards, the fibers were cleaned in the distilled water for 2 min. To obtain a catalytic surface, fibers were activated in a solution containing $PdCl_2$ and HCl. At the end of this process, the fibers were rinsed in distilled water. The pre-reduction step was performed at 70 °C for 5 min under ultrasonic vibrations in a solution consisting of 0.01 M $NiSO_4$ and 0.2 M NaH_2PO_2. The metallization process was conducted at 70 °C in a thermostatic vessel (200 mL solution) under ultrasonic vibration. The duration of the processes were 3, 5.5, 11, and 22 min. The solution for Ni-P deposition was composed of $NiSO_4$ (0.1 M), NaH_2PO_2 (0.2 M), glycine (0.21 M),

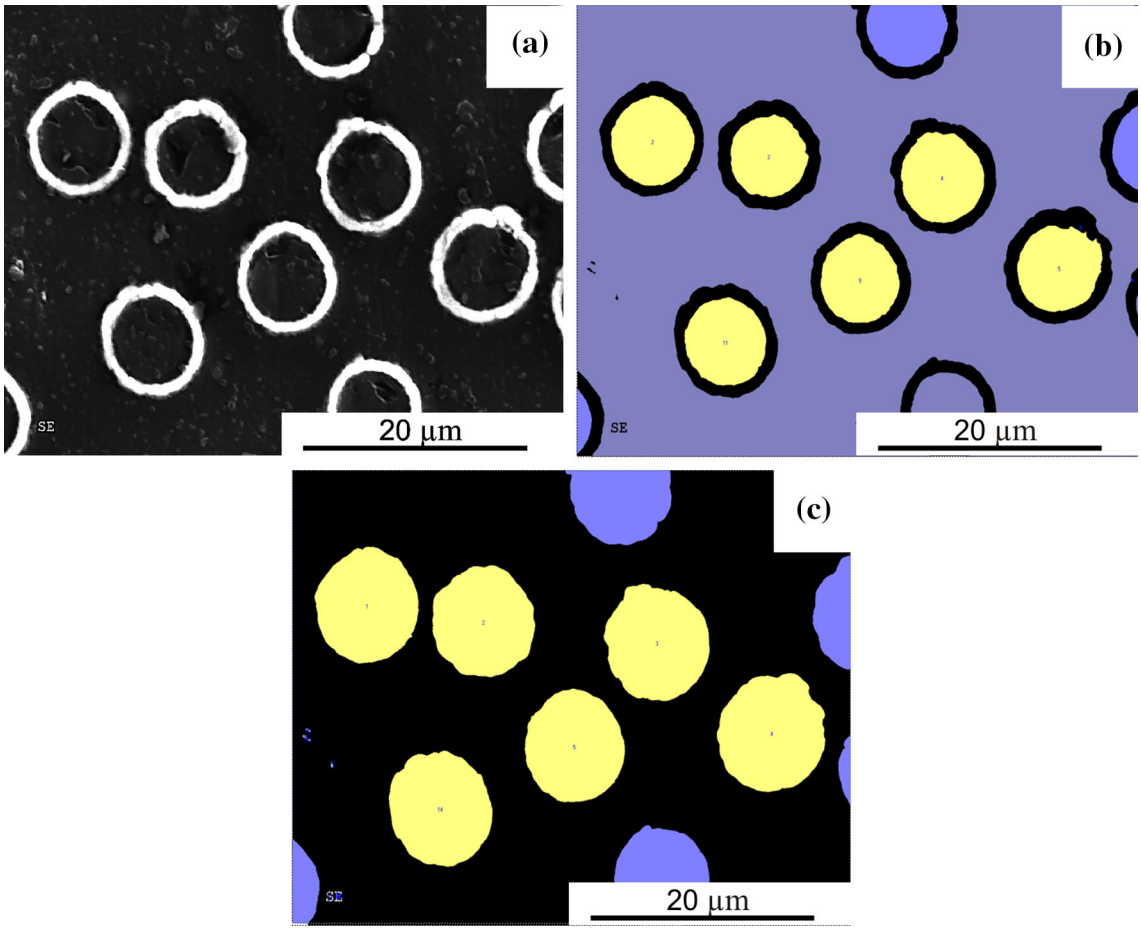

Fig. 1 Images of a cross section of the Ni-P coatings deposited on carbon fibers: (a) SEM image; (b) image of the measured fibers without coating; (c) with coating

and NaOH as a pH regulating additive (pH value was 8.5). Thiourea (0.2 mM) was added as the stabilizer, and cetyltrimethylammonium bromide (0.1 mM) was added as the surfactant.

The coated samples were examined by scanning electron microscopy (SEM) (Hitachi S5500 and Hitachi TM3000). First, coated fiber samples were embedded in epoxy resin, packing the fibers in a cuboidal mold. After curing, samples were polished and sputtered with a 4-nm thick Au layer to provide optimal conditions for microscopic observations. Then, obtained images were subjected to processing in a graphics program according to the procedure presented in Fig. 1. The thickness of the coatings was measured based on the images of the cross sections of the coated fibers (Fig. 1a) via measurements of the fiber and coated fiber diameters (Fig. 1b and c).Gray scale images were first treated with a median filter. Next, binarization at the threshold values was determined by the local minima on the gray level histogram. The resolution of the measurements provided by the Micrometer software was approximately 0.043 µm. This value corresponds to 1 pixel in the analyzed images. For thicker coatings, where sticking together of neighboring fibers occurred, only circle sectors were examined. The sticking regions were not taken into account in the measurements. The outer diameter of the fiber with coating was calculated from the measured circle sector area, taking into account the central angle. The obtained parameters were used to calculate thickness of the coating according to the following Eq 1:

$$h = \frac{d_2 - d_2'}{2}, \qquad \text{(Eq 1)}$$

where h is the coating thickness, d_2 is the diameter of the coated fiber, and d_2' is the diameter of the fiber.

To ensure that the measurements were based only on the cross sections of the coated fibers that were perpendicular to the surface of the sample, before investigation, the ratio of the maximal and minimal Ferret diameters of the fibers, (d_{max}) and (d_{min}), respectively, was analyzed. When the ratio deviated from unity by 5%, the fiber was rejected from further processing.

The results of the geometrical measurements were compared with the estimates based on the weight measurements performed with an analytical balance (0.0001 g accuracy). The latter were obtained using Eq 2:

$$h = \frac{D_o}{2}\left(\sqrt{1 + 0.2\frac{m_{Ni}}{m_C}} - 1\right), \qquad \text{(Eq 2)}$$

where h is the theoretical coating thickness (µm), D_o is the diameter of the uncoated fiber (7 µm), m_C is the mass of the uncoated bundle, m_{Ni} is the mass of the Ni-P coating obtained from the difference between the mass of the coated and uncoated bundles.

The morphology of the coatings was investigated starting from the central part (Fig. 2a) to provide characteristics for the

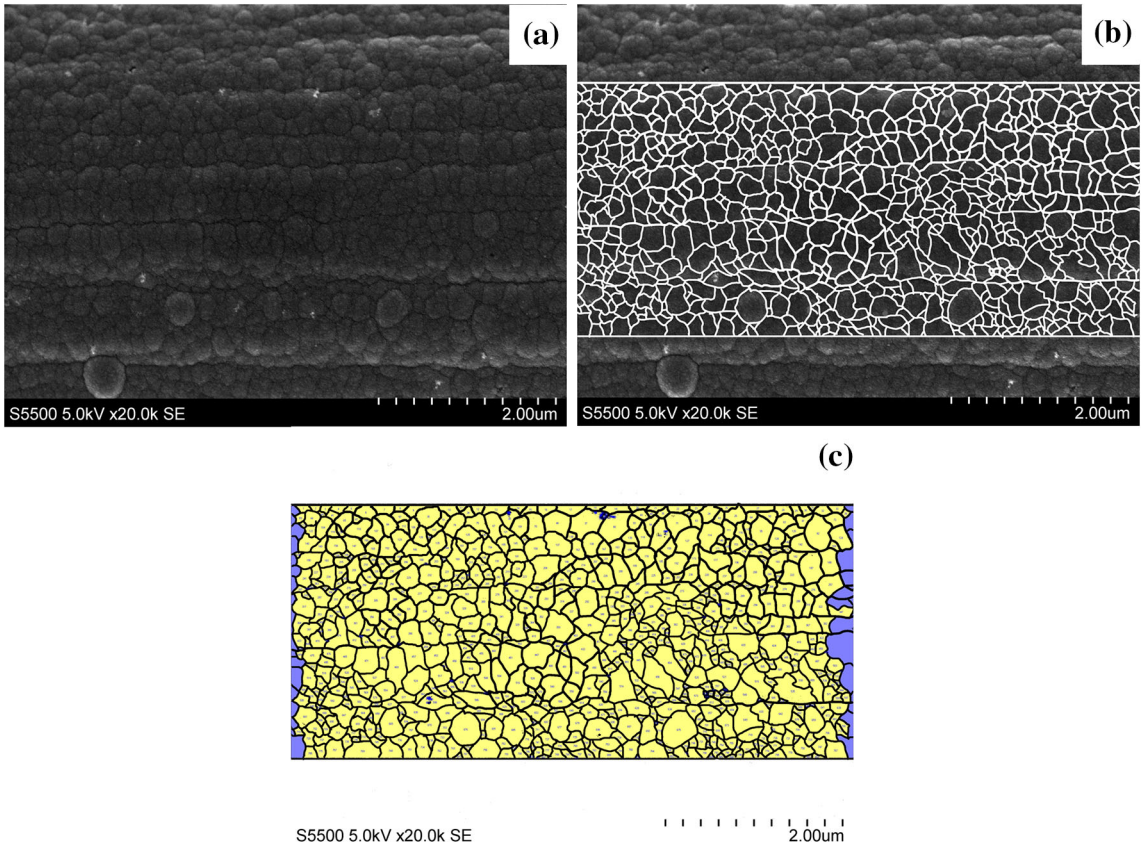

Fig. 2 Images of the coatings: (a) live image; (b) digitized to delineate bulges; (c) as analyzed

flattest fiber surface. Each hemisphere was outlined, as shown in Fig. 2(b). The images were analyzed in the Micrometer program. The results are shown in Fig. 2(c). For the description of the hemisphere diameter, the maximum Feret diameter (d_{max}) was used. Even on a non-perfectly perpendicular image plan, the max Feret diameter of a circle remains constant, in contrast to other parameters. Because the fiber/coated fiber section is almost circular, the diameter was assessed from the measurement of the section area. The total number of analyzed hemispheres for each sample was approximately 2000, and approximately 100 measurements of the coating thickness were made to provide adequate statistics. The procedure of the manual object boundaries selection was carefully examined and was conducted independently by 5 people The two outer layers were rejected, and the 3 middle results were averaged.

The mean values of the measured parameters were analyzed, and the coefficient of variation of the maximum Feret diameter was given by Eq 3

$$CV = \frac{SD}{\chi} \cdot 100\%, \qquad \text{(Eq 3)}$$

where SD is the standard deviation and x is the arithmetic average.

3. Results and Discussion

Representative SEM images of the cross sections of the Ni-P-coated carbon fibers after different times of metallization are presented in Fig. 3. Metallization of 11 min preserves the separation of fibers. At a processing time of 22 min, the coatings connect single fibers in the groups, as shown in Fig. 4, which is a highly undesirable effect in the case of fibers for reinforcement in metal matrix composites because the reduced space between coated fibers makes the process of infiltration by liquid metal difficult (Ref 20).

Additionally, the results achieved by the image analysis indicated that joining fibers into groups can disturb the proper coating thickness measurement. Theoretical calculations based on the quantity of deposited nickel are also improper because of the fiber agglomeration. Many fibers share one coating, and new layers of nickel phosphorous grow only on the surfaces not covered by other fibers.

The results of the coating thickness measurements are plotted in Fig. 5 against the metallization time. The thickness increases at a constant rate of 1.5 nm/s. This is an interesting finding because a constant rate of thickness growth can be achieved only under conditions of an accelerated total deposition rate of Ni-P. The results reported here prove that to achieve a specific deposition rate, the deposited mass per surface area of the coating must remain constant during the metallization process.

Furthermore, for metallization time up to 11 min, the results agree with the estimates based on the weight measurements. The values were nearly the same or stayed within the range of the standard deviation (SD) values, as in the case of 11 min metallization. In contrast to the theoretical calculations (using Eq 2), the image analysis allows calculation of the SD values. Utilizing this parameter, it was possible to draw conclusions about the diversity of the coating thickness in the range of the fiber, which is important in optimization of the coating thickness for polymer and metal matrix composites.

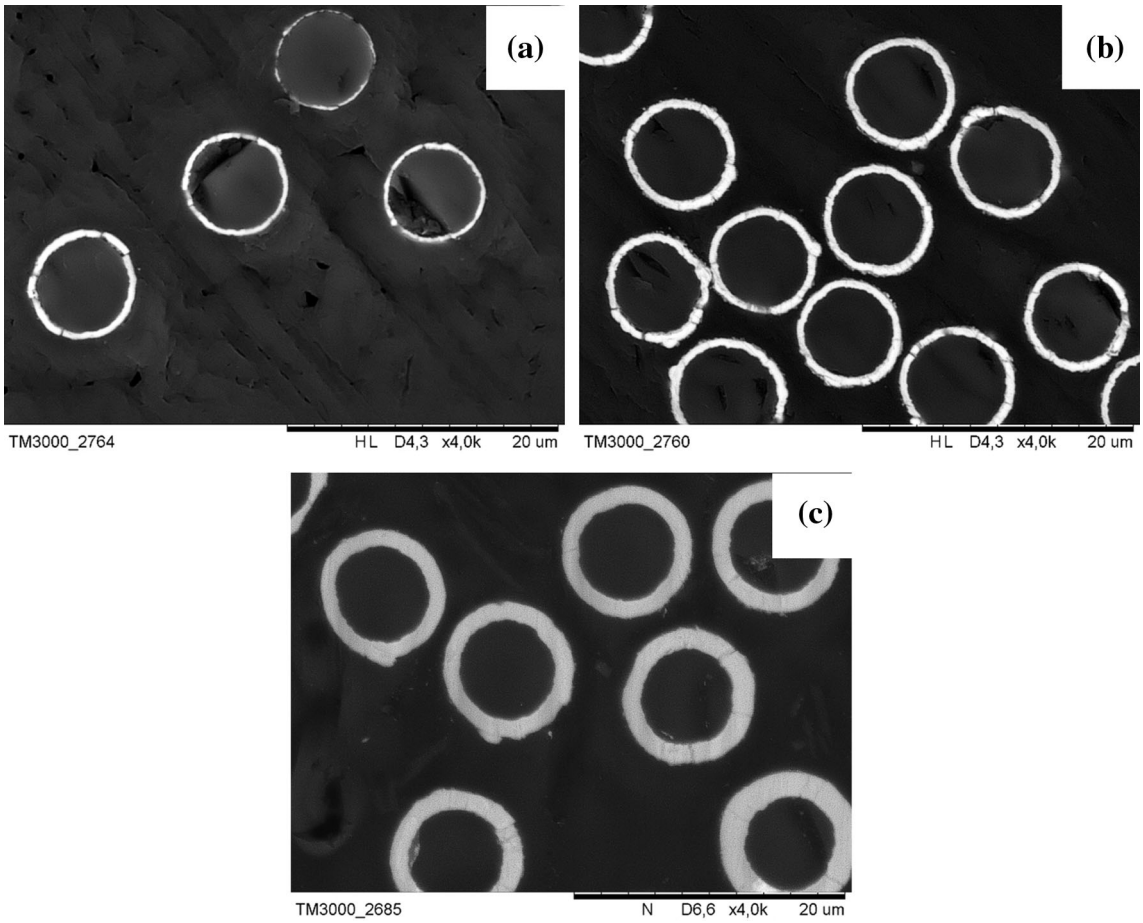

Fig. 3 Images of the cross sections of the coatings (white rings) after metallization for: (a) 3 min; b) 5.5 min; (c) 11 min

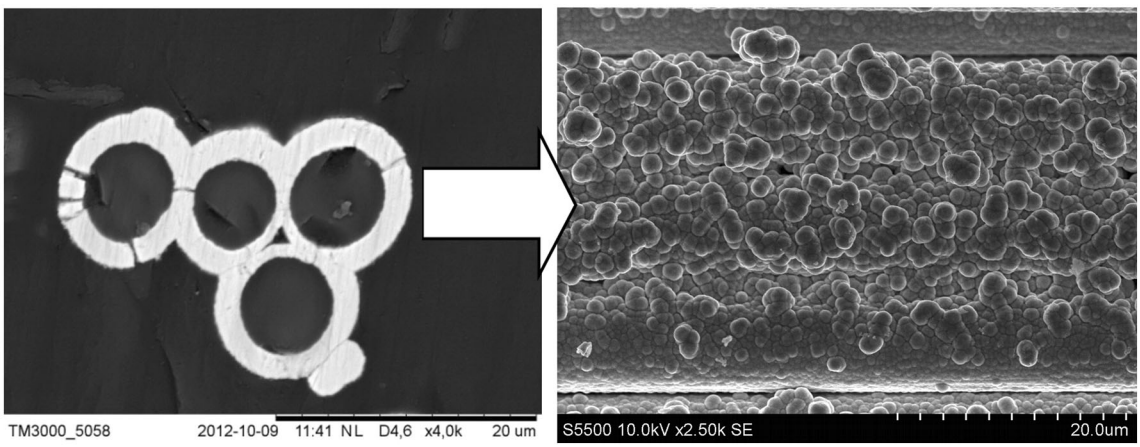

Fig. 4 Images of the coated carbon fibers after 22 min of metallization: (a) cross section; (b) surface of three joined fibers

The image analysis showed an increase in the coating thickness for 22 min metallization, but the thickness of the coatings was higher in comparison to the weight measurements of the nickel deposition, which can be explained by the non-uniform coating thickness distribution that was confirmed by the SD values. Fibers joined into group have thicker coatings outside of the bundles than inside. On the other hand, the weight measurements are relevant to the whole surface area of the fibers. Therefore, in practical applications of the coated fibers, i.e., for metal matrix composites (MMC), thick coatings or 1 or 1.6 μm are not advisable because of the formation of brittle phases when dissolving the coating in the matrix (Ref 21).

Considering this fact, for practical applications, the optimal time for the process is determined in a way that ensures a coating that is not too thick. Although the developed method can be applied for well-separated and distant fibers with thick coatings, in practice, due to technological reasons, carbon fibers are formed in tight bundles. This configuration limits their mobility inside the group of fibers. Moreover, a large thickness causes cracking of the coatings, even during the metallization process.

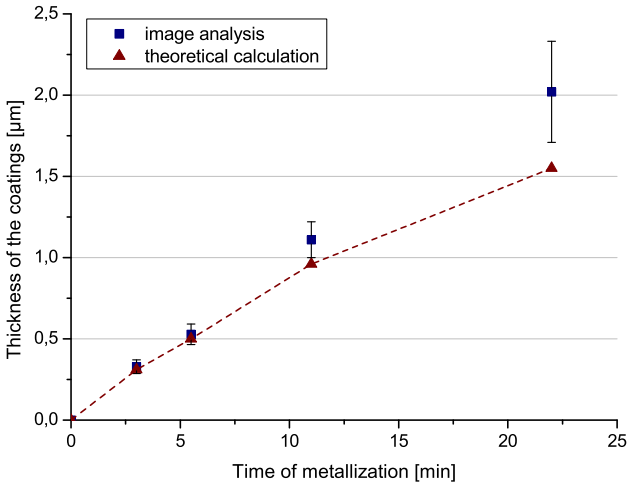

Fig. 5 The measured average thickness and estimates based on the weight measurements. The SD of the coating thickness is used to determine the error bars

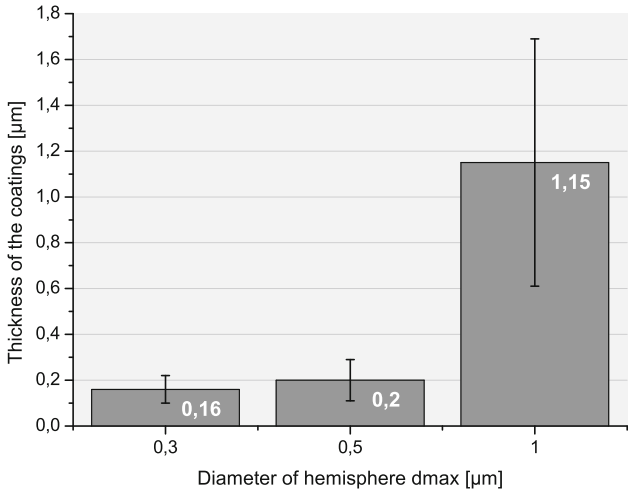

Fig. 7 Diameters of the hemispheres measured by image analysis for the coatings with thicknesses of 0.3, 0.5, and 1 µm

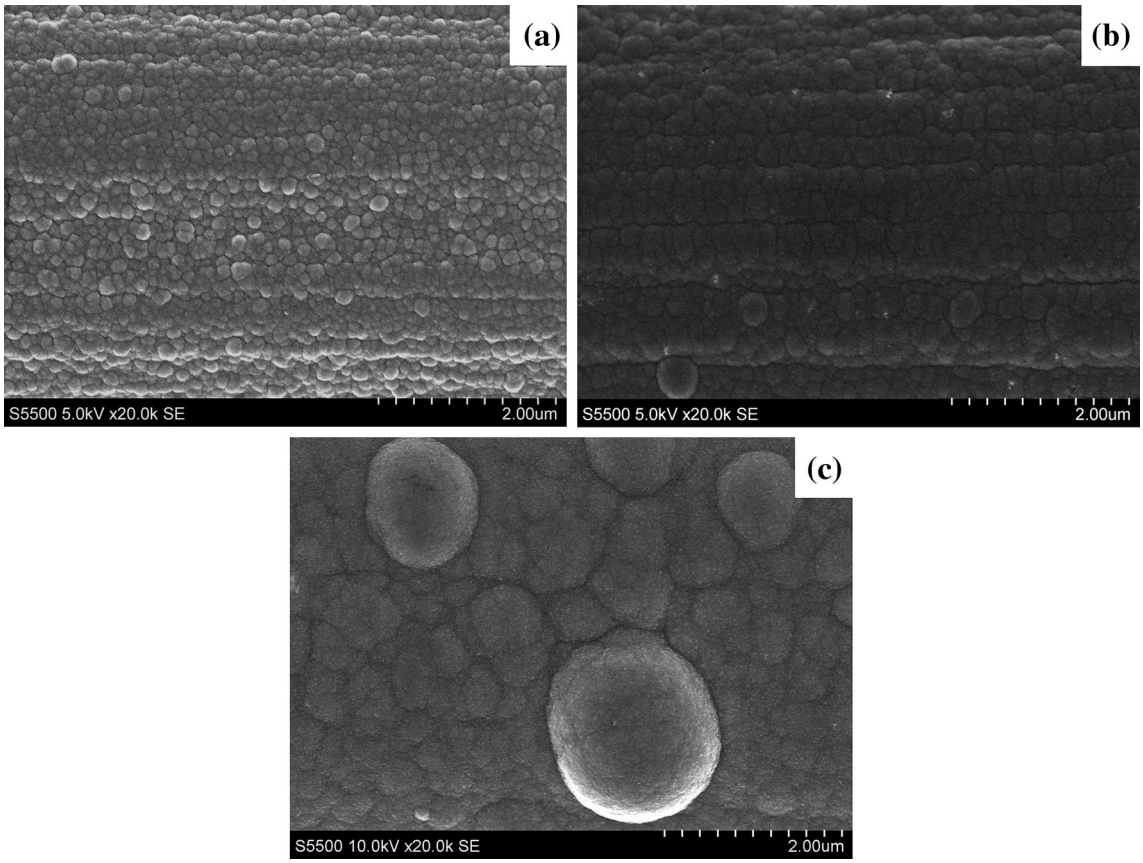

Fig. 6 Morphology of the Ni-P coatings after different times of metallization: (a) 3 min; (b) 5.5 min; (c) 11 min

The duration of the metallization process influences the morphology of Ni-P coatings (Ref 20). Because of the sticking of the fibers after coating for 22 min (Fig. 4a) and the high SD parameter, analysis of the diameters of the hemispheres was limited to coatings deposited up to 11 min. A high SD indicates a large difference in the thickness of the coatings inside the bundle, which can significantly affect the morphology. Figure 6 shows representative morphologies after 3, 5, and 11 min of metallization. Changes in the diameter of the hemispheres are clear. However, these changes are non-linear as a function of the coating thickness—see the results in Fig. 7. At 3 and 5.5 min of metallization, no substantial difference in hemisphere diameters is observed. A large increase in the diameter and in the standard deviation was found for the 11 min sample. The results suggest that the hemispheres play a dominant role in the coating growth, as described by Jahazi and Jalilian (Ref 15, 21).

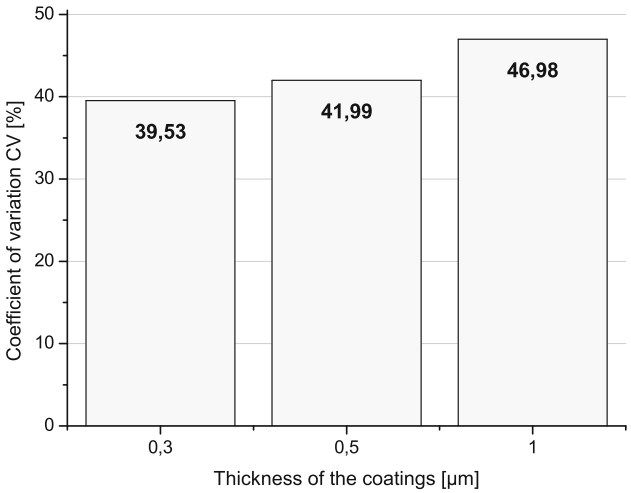

Fig. 8 Non-homogeneity of the coating morphology described with coefficients of variation CV of diameters of the surface bulges

The non-homogeneity of the coating morphology, as described using the coefficient of variation (CV), is depicted Fig. 8. The highest value of CV was measured for the coating with a 1-µm thickness. Histograms of the hemisphere diameters are shown in Fig. 9. A log axis has been used for the hemisphere diameters to allow presentation of the significantly different samples on the same axis. Moreover, the obtained diameter distributions are reasonably well-approximated by log-normal distributions (dotted lines in Fig. 9).

The histograms shown in Figure 9 indicate that the diameter distribution function for the lowest coating thickness (0.3 and 0.5 µm) is relatively narrow, with the most frequent values in the range 200-250 nm. The distribution function widens for sample with a 1.0-µm coating thickness, but the unbiased measure of dispersion, the CV, does not grow as rapidly.

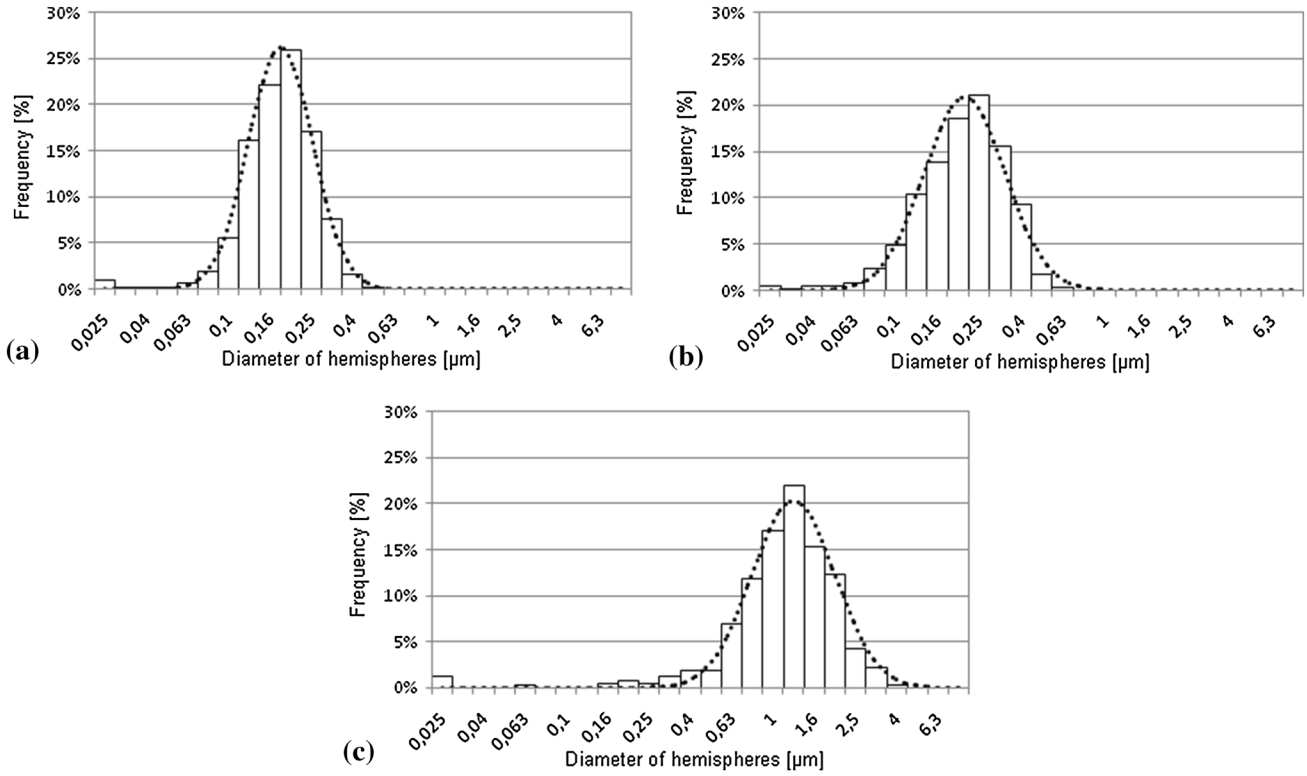

Fig. 9 Experimental histograms of the relative frequency of the hemisphere diameters for the coatings: (a) 0.3; (b) 0.5; and (c) 1 µm, log-normal distribution model (dotted line)

4. Conclusions

The quantitative image analyses conducted in this study lead to the following conclusions:

- Application of quantitative image analysis and advanced electron imaging techniques allows assessment of the diversity in the coating thickness between individual fibers in the bundle.
- Estimates of the coating thickness based on weight measurements provide good results only for relatively thin coatings with thickness below 1 μm.
- Profound changes in the morphology of the coatings occur at the thickness of 1.0 μm with the size of surface bulges becoming significantly diverse.

Finally, the results presented in this report provide tools for optimizing the thickness of the coatings obtained by electroless metallization. In particular, the thickness of the coating or metal matrix composites can be better controlled to prevent coating overgrowth. Moreover, because the Ni-P, Ni, and Cu reactive coatings in most studied cases dissolve when in contact with liquid aluminum alloys (Ref 16, 21, 22), the developed method can also help to control the formation of brittle phases during the infiltration process through the adjustment of the coating thickness and the mechanical properties of the aluminum alloys matrix composite.

Acknowledgments

This study was supported by the Polish Ministry of Science and Higher Education and by DFG in Germany as the Polish-German Bilateral Project "3D-textile reinforced Al-matrix composites (3D-CF/Al-MMC) for complex stressed components in automobile applications and mechanical engineering" No. 769/N-DFG/2010/0.

References

1. R.C. Agarwala and V. Agarwala, Electroless Alloy/Composite Coatings: A Review, *Sadhana*, 2003, **28**(3–4), p 475–493
2. M. Schlesinger and M. Paunovic, *Modern Electroplating: Chapter 3 Electrodeposition of Nickel*, Wiley, New York, 2010
3. K. Krishnan, S. John, K.N. Srinivasan, J. Praveen, M. Ganesan, and P.M. Kavimani, An Overall Aspects of Electroless Ni-P Depositions—A Review Article, *Metall. Mater. Trans. A*, 2006, **37A**, p 1917–1926
4. G.O. Mallory, J.B. Hajdu, Ed., Electroless Plating: Fundamentals and Applications, AESF, Publishing, Orlando, 1990
5. C. Huang and W. Mo, The Effect of Attached Fragments on Dense Layer on Electroless NiP Deposition on the Electromagnetic Interference Shielding Effectiveness of Carbon Fibre/Acrylonitrile-Butadiene-Styrene Composites, *Surf. Coat. Technol.*, 2002, **154**, p 55–64
6. C. Huang and T. Chiou, The Effect of Reprocessing on the EMI, Shielding Effectiveness of Conductive Fibre Reinforced ABS Composites, *J. Eur. Polym.*, 1998, **34**(1), p 37–43
7. C. Huang and J. Pai, Studies on Processing Parameters and Thermal Stability of ENCF/ABS Composites for EMI, Shielding, *J. Appl. Polym. Sci.*, 1997, **63**(1), p 115–123
8. C. Huang and J. Pai, Optimum Conditions of Electroless Nickel Plating on Carbon Fibres for EMI, Shielding Effectiveness of ENCF/ABS Composites, *J. Eur. Polym.*, 1998, **34**(2), p 261–267
9. G. Lu, X. Li, and H. Jinag, Electrical and Shielding Properties of ABS Resin Filled with Nickel-Coated Carbon Fibers, *Compos. Sci. Technol*, 1996, **56**(2), p 193–200
10. W. Hufenbach, M. Gude, A. Czulak, A. Gruhl, P. Malczyk, and F. Engelmann, *Carbon Fibre Light Metal Composites Manufactured with Gas Pressure Infiltration Methods*, Wroclaw, Prod. Eng. Innov. Technol. Future, 2011, p 91–105
11. W. Hufenbach, A. Czulak, P. Malczyk, A. Gruhl, Kompozyty na osnowie metali lekkich. Innowacyjne kierunki rozwoju nowoczesnych konstrukcji (Light Metal Matrix Composites. Innovative Directions of Development of Modern Constructions), Projektowanie i Konstrukcje, 11, 2011, p 14–19
12. A. Dolata, M. Dyzia, and J. Śleziona, Al/CF Composites Obtained by Infiltration Method, *Composite*, 2011, **4**, p 310–316
13. P. Morgan, *Carbon Fibers and Their Composites, Chapter 16: Carbon Fibers in Metal Matrices*, CRC Press, Boca Raton, 2005, p 629–656
14. T.P.D. Rajan, R.M. Pillai, and B.C. Pai, Review: Reinforcement Coatings and Interfaces in Aluminium Metal Matrix Composites, *J. Mater. Sci.*, 1998, **33**, p 3491–3503
15. M. Jahazi and F. Jalilian, The Influence of Thermochemical Treatments on Interface Quality and Properties of Copper/Carbon-Fibre Composites, *Compos. Sci. Technol.*, 1999, **59**, p 1969–1975
16. J. Rams, A. Urena, M.D. Escalera, and M. Sanchez, Electroless Nickel Coated Short Carbon Fibres in Aluminium Matrix Composites, *Compos.: Part A*, 2007, **38**, p 566–575
17. P. Soo-Jin and J. Ui-Sin, X-ray Diffraction and X-ray Photoelectron Spectroscopy Studies of Ni-P Deposited onto Carbon Fiber Surfaces: Impact Properties of a Carbon-Fiber-Reinforced Matrix, *J. Colloid Interface Sci.*, 2003, **263**(1), p 170–176
18. S. Ziyuan, W. Xuezhi, and D. Zhimin, The Study of Electroless Deposition of Nickel on Graphite Fibers, *Appl. Surf. Sci.*, 1999, **140**, p 106–110
19. S.B. Sharma, R.C. Agarwala, V. Agarwala, and K.G. Satyanarayana, Characterization of Carbon Fabric Coated with Ni-P and Ni-P-ZrO_2-Al_2O_3 by Electroless Technique, *J. Mater. Sci.*, 2002, **37**(24), p 5247–5254
20. H.A. Sorkhabi and S.H. Rafizadeh, Effect of Coating Time and Heat Treatment on Structure and Corrosion Characteristics of Electroless Ni-P Alloy Deposits, *Surf. Coat. Technol.*, 2004, **176**, p 318–326
21. S. Abraham, B.C. Pai, K.G. Satyanarayana, and V.K. Vaidyan, Studies on Nickel Coated Carbon Fibres and Their Composites, *J. Mater. Sci.*, 1990, **25**, p 2839–2845
22. A. Urena, J. Rams, M.D. Escalera, and M. Sanchez, Effect of Copper Electroless Coatings on the Interaction Between a Molten Al-Si-Mg Alloy and Coated Short Carbon Fibres, *Compos. Part A*, 2007, **38**, p 1947–1956